ELSEVIER

Physics of the Earth and Planetary Interiors 108 (1998) 219–234

PHYSICS OF THE EARTH AND PLANETARY INTERIORS

Modelling planetary dynamics by using the temperature at the core–mantle boundary as a control variable: effects of rheological layering on mantle heat transport

Arie P. van den Berg [a,*], David A. Yuen [b,1]

[a] *Dept. of Theoretical Geophysics, Institute of Earth Sciences, Utrecht University, 3508 TA Utrecht, Netherlands*
[b] *Dept. of Geology and Geophysics, Minnesota Supercomputer Institute, University of Minnesota, Minneapolis, MN 55415-1227, USA*

Received 5 August 1997; revised 11 March 1998; accepted 27 March 1998

Abstract

In planetary convection, there has been a great emphasis laid on the usage of the Rayleigh number as a control parameter for describing the vigor of convection. However, realistic mantle rheology not only depends on temperature, pressure, strain-rate and composition, but also on the nature of the dominant creep mechanism, which varies with pressure and also with temperature. It is difficult to study the effects of varying influences from the convective strength without also changing the mantle flow law in the process. We have adopted the approach of using as the sole control parameter, the temperature at the core–mantle boundary, T_{CMB}, in modelling planetary dynamics with a composite non-Newtonian and Newtonian rheology, which is temperature-dependent in the upper mantle and both temperature- and pressure-dependent in the lower mantle. Increasing the T_{CMB} strengthens convective vigor and leads to a non-linear increase of averaged temperature, heat-flow and root-mean-squared velocity. The interior viscosity decreases strongly with T_{CMB} and internal heating due to radioactivity. A viscosity maximum is found in the horizontally averaged viscosity profile at a depth around 2000 km. This viscosity hill moves downward with diminishing amplitude in the face of increasing dissipation number and internal heating. The bottom third of the lower mantle appears to be superadiabatic as a consequence of the stiff lower-mantle rheology. The scaling relationship between the Nusselt (Nu) number and T_{CMB} shows a relatively insensitive increase of Nu with T_{CMB}. In terms of an effective Rayleigh number of the whole system, Ra_E, the power-law exponent of the Nu (Ra_E) relationship is very low, around 0.12. Strong pressure-dependence of lower-mantle rheology and its large volume relative to the entire mantle would induce a much lower cooling rate of the planet than previous models based on parameterized convection with a temperature-dependent viscosity.

Keywords: Convection; Rayleigh number; Rheology

1. Introduction

The rheology of terrestrial planetary mantles depends on many factors, such as temperature, pressure, strain-rate and composition. In the past 20 years with the growing popularity of parameterized convection (e.g., Mc Kenzie and Weiss, 1975; Sharpe and Peltier, 1978), much emphasis has been placed on temperature-dependent viscosity and its effects on thermal history (Spohn and Schubert, 1982), the regimes of finite amplitude convection (Solomatov

* Corresponding author. E-mail: berg@geo.uu.nl
[1] E-mail: davey@msi.umn.edu

0031-9201/98/$19.00
PII S0031-9201(98)00101-0

and Moresi, 1996). Yet the effects of pressure-dependence on mantle convection have been shown to be quite profound on the dynamics (Balachandar et al., 1992; Hansen et al., 1993; Zhang and Yuen, 1995, 1996; Bunge et al., 1996, 1997). The effects of rheological stratification on mantle flows have been studied by van den Berg et al. (1991), van Keken et al. (1992, 1993) and van den Berg and Yuen (1996).

Moreover, there are ample evidences that the mantle is stratified rheologically with the creep laws constantly changing with depth from linear to non-linear in the top 400 km of the mantle and back again to non-linear in the transition zone and to Newtonian in the lower mantle (Karato and Wu, 1993; Karato, 1992; Karato et al., 1995; Karato, 1997). van den Berg and Yuen (1996) have pointed out the profound effects from the lower-mantle pressure dependence of the viscosity on the overall rheological structure of a composite Newtonian–non-Newtonian temperature- and pressure-dependent rheology. Because of these depth variations of the flow laws, it is really becoming difficult to have a good handle on the effects of varying the Rayleigh (Ra) number and not changing the rheological law in the process. The Ra number, in the traditional sense, is a dimensionless quantity based on global quantities, such as the mantle thickness, average viscosity and thermal conductivity. Machetel and Weber (1991) and Machetel et al. (1995) have advocated the usage of physical dimensional quantities as a means of characterizing mantle convection, since the dimensionless parameters, such as the dissipation number and Ra number, are coupled. For the Earth and Venus, the global Ra number is, in fact, dominated by the creep law of the lower mantle, which has a strong pressure-dependence, as inferred from the steep melting slopes of perovskites and other lower mantle constituents (Zerr and Boehler, 1993, 1994; Shen and Lazor, 1995; Holland and Ahrens, 1997).

In this paper, we will illustrate another vantage view in parameter variation by presenting results from a two-dimensional cartesian model in which we will vary the temperature at the core–mantle boundary, T_{CMB}, as the control parameter. These calculations will be conducted within the framework of a composite Newtonian and non-Newtonian rheology (van den Berg et al., 1993), in which the nature of the creep law varies with depth. We will show how the common output such as average temperature, viscosity profiles, would vary with T_{CMB}, as well as showing how the heat-transfer relationship as a function of convective vigor, would be influenced by this type of temperature- pressure- and strain-rate dependent rheology. We will also discuss how this rheology would impact on the nature of adiabaticity in the deep mantle.

2. Model description

2.1. Model configuration and rheology

We have studied the Earth's mantle as a first example. A 2-D rectangular model with a depth of 3000 km and aspect-ratio 2.5 has been used for the sake of simplicity and computational costs. This is displayed in Fig. 1. We have put in a rheological interface at a depth of 670 km to separate the upper- and lower-mantles. There are no phase transitions in this model. This composite rheological model has a Newtonian and non-Newtonian rheology with only temperature-dependence in the upper mantle, while the lower mantle's Newtonian and non-Newtonian rheology has temperature and pressure dependencies. We note explicitly that both linear (Newtonian) and non-linear (non-Newtonian) creep laws operate simultaneously. Their relative contribution to the overall creep efficiency is governed by the transition stress and the style of convection (van den Berg et al., 1993). A constitutive relationship involving both types of strain-rate dependencies has been employed:

$$e_{ij} = \left[A_1(p,T) + A_2(p,T)\tau^{n-1} \right] \tau_{ij} \qquad (1)$$

where the Newtonian and power-law components are

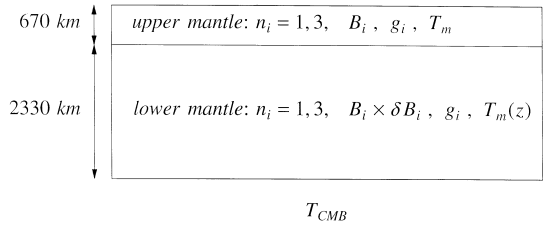

Fig. 1. Configuration of the 2-D model showing the rheological layering of the upper and lower mantle, characterized by the power-law index n_i, the viscosity prefactor B_i and the melting temperature T_{m}, for both active creep mechanisms $i = 1, 2$.

denoted by subscripts 1 and 2. In Table 2, we give the definitions of the symbols.

$$\eta(p,T,\tau) = \left[A_1(p,T) + A_2(p,T)\tau^{n-1}\right]^{-1} \quad (2)$$

In Eq. (2), the terms in A_i represent the inverse viscosities $1/\eta_i$ corresponding to the individual creep components of the strain-rate in Eq. (1). The same composite rheology has been used in the work of van den Berg and Yuen (1997) for studying the effects of viscous dissipation on lubricating the lithospheric plates and also in the work of van den Berg and Yuen (1996) to study the transition in the predominance from power-law creep to the Newtonian creep mechanism with the decreasing vigor of convection. A simpler version of the composite rheology in Eq. (1) with only temperature dependence in the viscosity components A_i (Eq. (2)) was applied in the work of van den Berg et al. (1995), in analysing the spatial distributions in the effective viscosity by both stress and temperature fluctuations. Earlier in the work of van den Berg et al. (1993) a composite model where A_i is independent of both p and T was used to investigate the style of convection in models with a composite rheology.

For the pressure and temperature dependence in the present rheological model, we have used a parameterization based on the pressure dependent melting temperature of mantle material $T_m(p)$, expressed in the homologous temperature, T_m/T (Weertman and Weertman, 1975; van Keken et al., 1994; van Keken and Yuen, 1995; van den Berg and Yuen, 1996, 1997). We used experimental extrapolations of the melting temperature for lower mantle perovskite to span the values of T_m varying between 2500 K at the top of the lower mantle and 8000 K at the CMB (Zerr and Boehler, 1993, 1994). We used a uniform value of T_m throughout the upper mantle. The viscosity components η_i, $i = 1, 2$ are defined as,

$$\eta_i(p,T) = B_i \exp\left[\frac{g_i T_m(p)}{T_+ + T}\right]\tau^{1-n_i} \quad (3)$$

The temperature shift T_+, which effects the rheology mainly at shallow depth, effectively replaces the cold brittle top layer by a ductile viscous material. The Newtonian and power-law creep components show different pressure and temperature dependence, controlled by the respective activation energy and activation volumes, which have different values for both mechanisms (Ranalli, 1995). Thus, the two flow mechanisms dominate creep flow in the mantle under different p, T conditions (Karato and Wu, 1993). In particular, since the activation parameters of dislocation creep are larger than those of Newtonian diffusion creep, non-Newtonian dislocation creep is pre-dominant in the shallow upper mantle and Newtonian creep is dominant at deeper levels, especially in the lower mantle (Karato et al., 1995). In line with this, we have chosen the Weertman coefficients in the ratio $r = g_1/g_2 = 1/3$ and $g_2 = 5$. This results in a faster increase with depth of the power-law viscosity compared to the Newtonian viscosity. The values for g_i and the slope of the melting curve dT_m/dz are equivalent with an activation volume for power-law creep in the lower mantle $V_2 = 2.5$ cm^3/mol. The predominance of either one of the creep mechanisms can be expressed in terms of the transition stress τ_t (Parmentier et al., 1976; van den Berg et al., 1993). When the local stress is smaller than the temperature and pressure dependent transition stress, the flow will be mainly Newtonian. For stress levels higher than τ_t power-law creep will dominate the flow. By equating the strain-rate components in Eq. (1), we can solve for the transition stress, which is both temperature- and pressure-dependent.

$$\tau_t^{n-1} = \frac{B_2}{B_1}\exp\left[(1-r)\frac{g_2 T_m(p)}{T_+ + T}\right] \quad (4)$$

For values $r < 1$, the transition stress shows a similar pressure and temperature dependence as the individual viscosity components, η_i.

The viscosity prefactors B_i were defined as depth dependent properties. A uniform distribution was used with different values for the upper and lower mantle. We applied a discontinuous increase with depth across the upper/lower mantle interface at 670 km depth by factors $\delta B_1 = 10$, $\delta B_2 = 100$. A viscosity increase across the 670 km interface may be inferred from geoid inversion (King, 1995) and post-glacial rebound data (Lambeck et al., 1996). But more recent works by Mitrovica and Forte (1997) and Pari and Peltier (1996) have found very little viscosity contrast across the 670 km discontinuity, By using $\delta B_1/\delta B_2 < 1$ we apply an increase in the

transition stress across 670 km depth. This is in line with reports of a largely Newtonian rheological character of the lower mantle based on experimental data for perovskite analogue (Karato and Li, 1992) and from observations of seismic anisotropy (Karato et al., 1995). The viscosity prefactor values were determined from prescribed surface reference values of the two viscosity components expressed in the viscosity scale value η_0, given in Table 2. The ratio of η_{1R} and η_{2R} was chosen such that the flow in the shallow upper mantle is predominantly non-Newtonian (Karato and Wu, 1993).

The relative importance between pressure and temperature dependence can be quantified by the following parameter δ which enters the Arrhenius exponential argument in the rheological law.

$$\delta = \frac{\rho g d V^*}{E^*} \tag{5}$$

where d is the depth of the layer under consideration E^* and V^* are the equivalent activation energy and volume which can be expressed in the zero pressure intercept and the slope of the melting curve used in the definition of the homologous temperature, $E_i^* = Rg_i T_m(0)$, $V_i^* = Rg_i \mathrm{d}T_m/\mathrm{d}p$. Equivalent activation parameter values used in this study are listed for the upper and lower mantle separately in Table 1 with the corresponding values of δ.

For the lower mantle plausible values for activation energy and volume are given in the works of Sammis et al. (1977), O'Connell (1977) and Knittle and Jeanloz (1987). For upper mantle olivine activation parameters have been determined by Goetze and Kohlstedt (1973) ($E^* = 522$ kJ/mol) and Karato and Rubie (1997) ($V^* = 14 \times 10^{-6}$ m^{-6}). The resulting value of $\delta = 0.7$ illustrates the non-negligible influence of the pressure dependence for the upper mantle. We know in our study the lower mantle value of $\delta = 6$, whereas Christensen (1984) used a value of $\delta = 0.4$ for the whole mantle. van Keken et al. (1994) used values of δ for the lower mantle in the range 1–2. Steinbach and Yuen (1997) used a value of $\delta = 2.5$ for the lower mantle.

2.2. Model equations and numerical method

The model equations are based on the extended Boussinesq approximation (EBA) for an infinite Prandtl number fluid (Steinbach et al., 1989; Ita and King, 1994; Balachandar et al., 1996). We applied a non-dimensionalization scheme defined by the following scale values, numerical values are given in Table 2: spatial scale, $x_0 = h$ equal to the depth of the layer, time scale, $t_0 = h^2/\kappa$, equal to the heat diffusion time scale for the whole layer. The temperature difference across the layer, ΔT is used as the temperature scale. For the viscosity scale η_0 we use a reference value, such that the non-dimensional volume averaged effective viscosity will be close to unity. All other scale values have been derived from the space, time and viscosity scale values in a consistent way. The model equations in non-dimensional form are:

$$\partial_j u_j = 0 \tag{6.a}$$

$$-\partial_i \Delta p + \partial_j \tau_{ij} = \alpha \mathrm{Ra} T \delta_{i3} \tag{6.b}$$

$$\frac{\partial T}{\partial t} + u_j \partial_j T - \partial_j \partial_j T = \alpha D w (T + T_0) + \frac{D}{\mathrm{Ra}} \Phi + R \tag{6.c}$$

Eq. (6.a) represent the incompressibility constraint of the extended Boussinesq model. The momentum equation is given in Eq. (6.b) and Eq. (6.c) is the energy equation. The special case with the dissipation number $D = 0$ represents the BA also investigated in our modelling experiments. The first term on the right hand side represents the effect of adia-

Table 1
Rheological activation parameters

	Newtonian creep		Non-Newtonian creep		
	E^* (kJ/mol)	V^* (m^{-6}/mol)	E^* (kJ/mol)	V^* (m^{-6}/mol)	δ
Upper mantle	35	0.0	104	0.0	0
Lower mantle	13	0.83×10^{-6}	38.1	2.5×10^{-6}	6

Table 2
Physical parameters

Symbol	Definition	Value	Unit
h	Depth of the mantle model	3×10^{6}	m
z	Cartesian depth coordinate aligned with gravity	–	–
z_1	Non-dimensional depth upper/lower mantle interface	0.223	–
p	Hydrostatic pressure	–	–
Δp	Hydrodynamic pressure	–	–
η	Effective dynamic viscosity	–	–
η_0	Viscosity scale value	10^{24}	Pa s
η_{1R}	Surface reference viscosity value (Newtonian creep)	1.166×10^{23}	Pa s
η_{2R}	Surface reference viscosity value (power-law creep)	1.587×10^{27}	Pa s
n_i	Power-law index η_i, $i=1,2$	1, 3	–
B_1	Viscosity prefactor for Newtonian creep	2.40×10^{21}	Pa s
B_2	Viscosity prefactor for power-law creep	1.71×10^{32}	Pa^3 s
δB_1	Lower/upper mantle prefactor ratio (Newtonian creep)	10	–
δB_2	Lower/upper mantle prefactor ratio (power-law creep)	100	–
g_1	Weertman coefficient for Newtonian flow	5/3	–
g_2	Weertman coefficient for power-law flow	5	–
r	$r=g_1/g_2$	1/3	–
T	Temperature	–	–
ΔT	Temperature difference across the mantle	–	K
T_0^{abs}	Dimensional surface temperature	273	K
T_0	Non-dimensional surface temperature $T_0=T_0^{abs}/\Delta T$	–	–
T_+	Temperature shift in the viscosity exponentials	800	K
$T_m(z)$	Depth dependent melting temperature	–	–
$T_m(z<z_1)$	Uniform upper mantle melting temperature	2500	K
$T_m(z=z_1)$	Top lower mantle value	2500	K
$T_m(z=1)$	Bottom lower mantle value	8000	K
u_i	Cartesian component of the velocity field	–	–
w	Vertical component of the velocity field	–	–
e_{ij}	Strain-rate tensor $e_{ij}=\partial_j u_i+\partial_i u_j$	–	–
e	$e=\lvert 1/2\, e_{ij}e_{ij}\rvert^{1/2}$ second invariant of e_{ij}	–	–
τ_{ij}	$\tau_{ij}=\eta e_{ij}$ deviatoric stress tensor	–	–
τ	$\tau=\lvert 1/2\,\tau_{ij}\tau_{ij}\rvert^{1/2}$ second invariant of τ_{ij}	–	–
Φ	Dissipation function $\Phi=\eta e^2$	–	–
R	Internal heating number $R=Hh^2/(c_p\kappa\Delta T)$	0, 5, 10	–
H	Rate of radiogenic heat generation	–	W kg^{-1}
ρ	Density	4000	kg m^3
κ	Thermal diffusivity	10^{-6}	m^2 s^{-1}
g	Gravity acceleration	9.8	m s^{-2}
c_p	Specific heat	1250	J kg^{-1} K^{-1}
α	Depth dependent thermal expansivity $\alpha(z)$, $\alpha(z)=\Delta\alpha[(1)/(c(1-z)+1)]^3$, $c=\Delta\alpha^{1/3}-1$	–	–
α_0	Surface value thermal expansivity	3×10^{-5}	K^{-1}
$\Delta\alpha$	Contrast across the mantle $\Delta\alpha=\alpha(0)/\alpha(1)$	5	–
Ra	Rayleigh number $Ra=\rho\alpha_0\Delta T g h^3/\kappa\eta_0$	–	–
D	Dissipation number $D=\alpha_0 gh/c_p$	0.7	–

batic heating and cooling, the second term corresponds to viscous dissipation and the last term gives the amount of radiogenic internal heating. A depth dependent thermal expansivity α with a contrast of five across the mantle has been used, defined in Table 2, (Chopelas and Boehler, 1992; Hansen and Yuen, 1994; Steinbach and Yuen, 1994). In this study, we will focus only on the steady-state solution because of the vast coverage of the parameter space this approach would permit.

Free slip and impermeable mechanical boundary conditions have been applied to all boundaries. Zero heat flux conditions apply on the vertical boundaries and prescribed temperature T_0^{abs} and $T_{CMB} = T_0^{abs} + \Delta T$ were used on the top and bottom boundary, respectively. Including the adiabatic heating term in the energy equation implies that the adiabatic temperature rise across the mantle is included in the modelling results in a self consistent way. Therefore, $\Delta T = T_{CMB} - T_0^{abs}$, used as a control variable in our models includes the adiabatic temperature rise across the mantle. This is illustrated in Fig. 2 where the different zones in the mantle are shown with different heat-transport characteristics, including the superadiabatic bottom lower mantle (zone A), and a well mixed middle mantle close to an adiabatic state (zone B). In this study, we define the Nusselt (Nu) number as the ratio of the heatflux through the top surface—adjusted for the contribution of the radiogenic internal heating—and the purely conductive heatflux in the absence of internal heating.

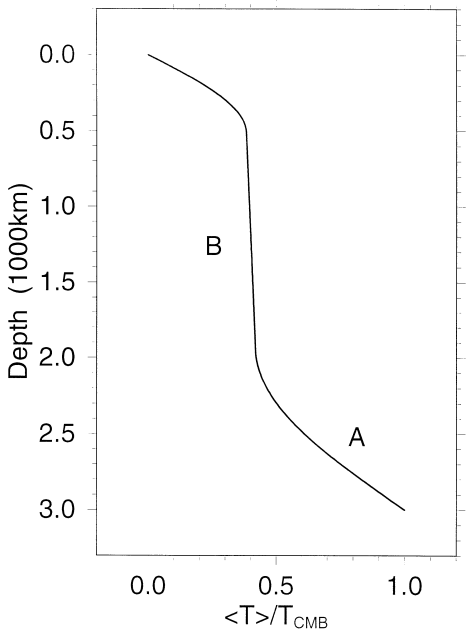

Fig. 2. Increase of temperature with depth in different mantle zones. T_{CMB} indicates temperature at the CMB and T_0 the temperature at the surface. The zones A and B denote respectively the superadiabatic zone in the deep mantle and the adiabatic core in the middle of the mantle.

We have solved the model Eqs. (6.a), (6.b) and (6.c) for steady-state solutions by dropping the partial derivative with respect to time in (6.c). We used a finite element method and Picard iteration, described in the work of van den Berg et al. (1993), to obtain solutions for the temperature and velocity fields. The combination of temperature dependent non-linear rheology and viscous dissipation included in the extended Boussinesq model complicates the convergence behavior of the Picard iteration scheme. Strong damping is required in the Picard iteration in order to stabilize the convergence. A relaxation factor of 0.1 appeared to be necessary to reach convergence to 1% in the solution vectors within 100 iterations (van den Berg et al., 1993).

Finite element meshes were used with up to 17,000 elements and 8500 nodal points, mesh refinement was used near the outer boundaries and near the rheological interface at the upper–lower mantle boundary. Element size varied between about 30 km in the mid-lower mantle and about 4 km near the vertical boundaries in the upper mantle.

3. Modelling results

In this section, we will present the steady-state results for a CMB temperature from 2273 K to 5573 K, different amounts of internal heating and both the EBA and the BA. Table 2 gives the basic physical parameters. We note that because of the complicated nature of the rheology, it is as easy to list the input parameters as for variable viscosity runs conducted in the past (e.g., Christensen, 1984). For further information, the reader can contact the authors. Plots of several resulting fields are given in Figs. 3 and 4. Fig. 3. shows results for internal heating number $R = 5$ and two different values of $T_{CMB} = 2773$ K, left-hand and $T_{CMB} = 5773$ K, right-hand column. Effective Ra number values, based on the volume averaged viscosity, for both cases are: $Ra_E = 9.12 \times 10^4$ and 1.65×10^6. The top row (a),(b) shows the non-dimensional temperature field. The thickness of the thermal boundary layers decreases for increasing T_{CMB}. Similarly the cold downwelling is more focussed for higher T_{CMB}. Frames (c),(d) show contours of the stream function illustrating the difference in velocity magnitude between the high viscos-

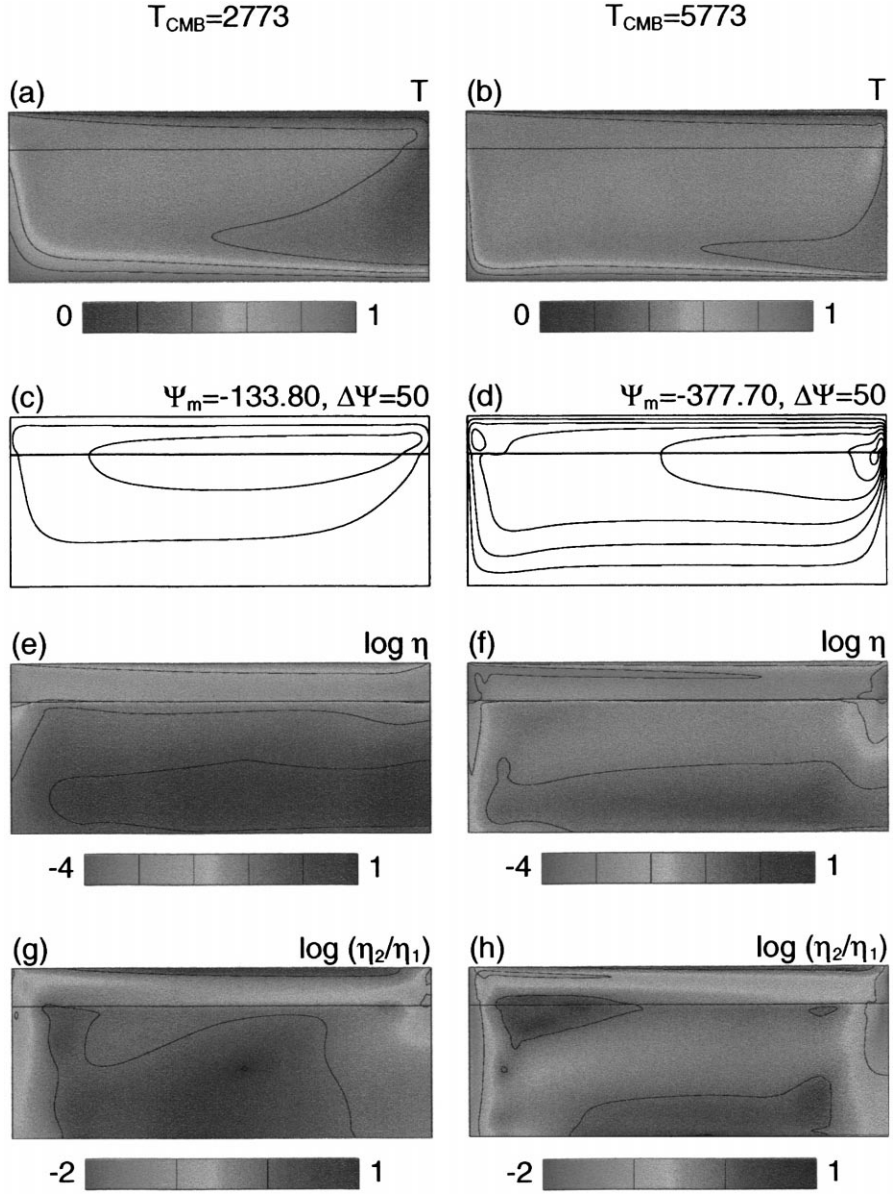

Fig. 3. Several fields corresponding to steady-state convection for internal heating mode $R = 5$ and for different values of T_{CMB}, $T_{CMB} = 2773$ K left hand column and $T_{CMB} = 5773$ K right hand column. (a),(b) show the temperature fields. (c),(d) show contours of the stream function. (e),(f) are the logarithmic effective viscosity fields. (g),(h) show the logarithmic ratio of the Newtonian and non-Newtonian viscosity components η_1 and η_2, illustrating the dominance of Newtonian creep in dark areas and power-law creep in light colored areas.

ity lower mantle and the more mobile upper mantle. The streamlines become more focussed for increasing T_{CMB} and the flow also becomes more plate-like near the top boundary. The streamlines especially show a strong focussing in the upper right-hand corner at the cold downwelling. This is related to the development of a low viscosity region in the upper mantle part of the cold downwelling illustrated in the effective viscosity plots shown in (e),(f). The viscosity plots illustrate the distinct layering in the viscos-

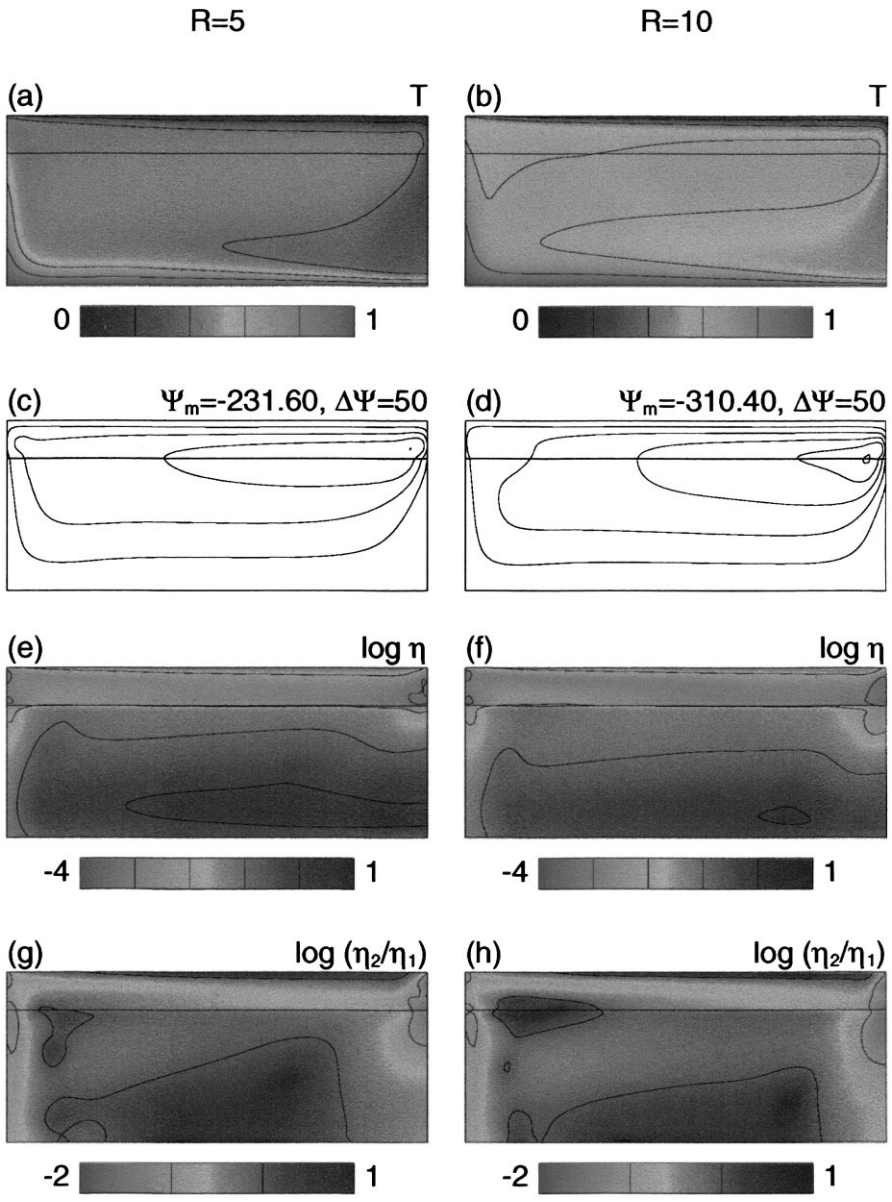

Fig. 4. The same fields as in Fig. 3 for fixed value $T_{CMB} = 3673$ K and for different values of the internal heating number, $R = 5$ left-hand column and $R = 10$ right-hand column.

ity between the mobile upper mantle and the high viscosity lower mantle. Regions of low viscosity in the lower mantle coincide with high strain-rate areas in the vertical limbs of the flow. Especially in the cold downwelling, the non-Newtonian flow component becomes dominant and reduces the viscosity. The combined effect of strain-rate weakening and weakening by the feed-back between viscous dissipation and strongly temperature dependent viscosity results in strong localized lubrication of downwelling plate motion (van den Berg and Yuen, 1997; Larsen and Yuen, 1997). These lubricating effects in the composite rheology make the use of ad-hoc weakness zones in models with temperature dependent

rheology unnecessary (Schmeling and Jacoby, 1981; Gurnis, 1989; King et al., 1992). Frames (g),(h) show the logarithmic ratio of the non-Newtonian and Newtonian viscosity contrasts. Regions where $\eta_2/\eta_1 < 1$ are characterized by a predominantly non-Newtonian flow field. The non-Newtonian character increases for increasing T_{CMB}. The upper mantle is largely non-Newtonian with the exception of the cold and stiff plate at the top-boundary. The lower mantle is predominantly Newtonian and this Newtonian character increases with depth in line with experimental data for perovskite analogue and observations of seismic anisotropy (Karato et al., 1995).

Fig. 4 shows the same fields as in Fig. 3 for a fixed value of $T_{CMB} = 3673$ K and two different internal heating modes, $R = 5$ left- and $R = 10$ right-hand column. The increase in internal heating results in an increase of the volume averaged temperature from 1831 K in (a) to 2296 K in (b). Effective Ra numbers are 2.79×10^5 (a) and 5.58×10^5. The viscosity decrease resulting from the increase in R is slightly smaller than the decrease shown in Fig. 3 resulting from increasing T_{CMB}. An increase in the internal temperature as shown in (a),(b), results in a decrease of the transition stress τ_t Eq. (4). This in turn will cause a shift in the dominant flow mechanism, which becomes more non-Newtonian as illustrated in Fig. 4g,h.

In Fig. 5, we summarize the steady-state results for the globally averaged viscosity $\langle\eta\rangle$, root-mean-squared velocity, heat-flow and globally averaged temperature $\langle T\rangle$ as a function of T_{CMB} for basal-heating ($R = 0$) to internally heated ($R = 5,\ 10$) situations. The effects of increasing T_{CMB} are to increase the averaged $\langle T\rangle$ in the mantle, to increase the velocity and the surface heat flow, as the flow becomes more vigorous. The effects of including dissipation in the EBA models over the BA models are to increase the overall temperature, decrease $\langle\eta\rangle$, increase the velocity and slightly increase the heat flow, in base heated mode and slightly decrease it for internally heated models. The effects of internal heating are to increase the averaged temperature, decrease $\langle\eta\rangle$, increase the velocity and the heat flow, as convective vigor is enhanced. An increase of a couple of thousand degrees in T_{CMB} can cause drastic differences in the flow regime. We note that averaged mantle viscosity of around 10^{23} Pa s is attained for models with reasonable internal heating ($R = 10$) and T_{CMB} between 3000 and 4000 K. This is in contrast to the basal heated models ($R = 0$) in which $\langle\eta\rangle$ exceeds 10^{24} Pa s. For reasonable geophysical predictions involving mantle viscosity (e.g., Mitrovica and Forte, 1997), some amount of internal heating seems to be needed.

In Fig. 6 we display the depth profiles of the horizontally averaged second invariant of the stress tensor $\langle\tau\rangle$ (a), of the viscosity $\langle\eta\rangle$ (b), of the temperature $\langle T\rangle$ (c), and the horizontal velocity in the center of the box U_C (d). The T_{CMB} is taken to be 3673 K. Much larger stresses are developed in the lower mantle because of the depth-dependent rheology (van Keken and Yuen, 1995; van den Berg and Yuen, 1996). The effects of internal heating are to decrease the stress levels and the viscosity but to increase $\langle T\rangle$. The central surface velocities are enhanced by the amount of internal heating and increased by dissipation for basal heating and decreased for higher rates of internal heating. Extended-Boussinesq models have higher interior temperatures than the Boussinesq models. Because of the variable-property nature of mantle rheology, the thermal–mechanical structure in the mantle is influenced by the dissipation number and the amount of internal heating. Constraints on the thermal–mechanical structure of the whole mantle have previously been made for variable viscosity, using the mean-field theory (Yuen and Zhang, 1989).

For constant viscosity convection the interior of EBA and anelastic compressive convection is adiabatic (Jarvis and Mc Kenzie, 1980; Machetel and Yuen, 1989; Steinbach et al., 1989). From mean-field calculations Quareni et al. (1986) have found that the mean temperature profile can deviate from the adiabat from the effects of depth-dependent viscosity. This was confirmed by 2-D solutions by van Keken et al. (1994) and 3-D calculations by Balachandar et al. (1992). Recently, Stacey (1997) has deduced from the PREM model (Dziewonski and Anderson, 1981) that the bottom 700 km of the lower mantle may be superadiabatic. Similar conclusions using first-principles quantum mechanics and the PREM model have also been reached (Wentzcovitch and Karato, personal communication, 1998). In Fig. 7, we plot the quantity $\beta(z)$, which represents the difference between $\mathrm{d}\langle T\rangle/\mathrm{d}z$ and the adiabatic gra-

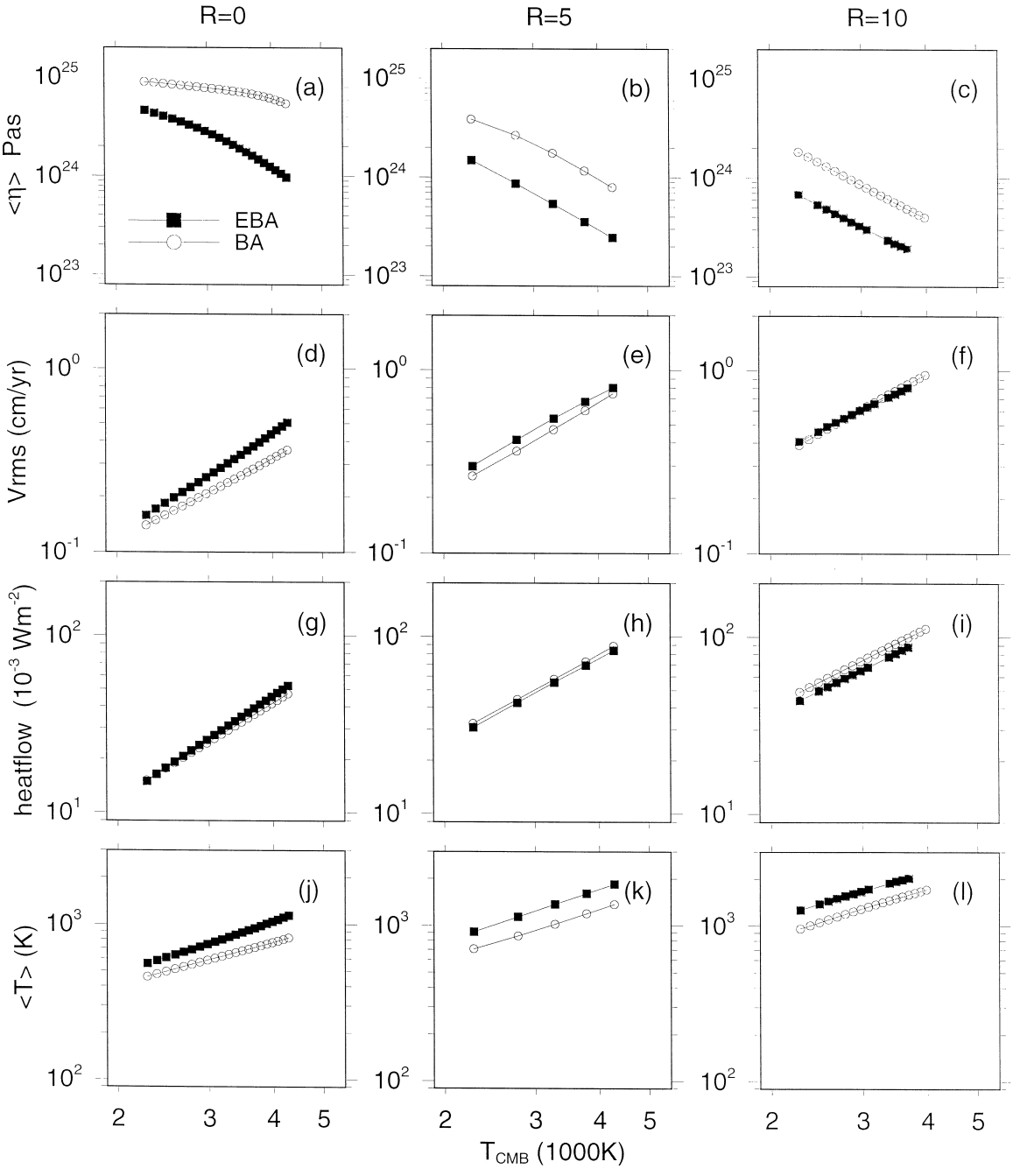

Fig. 5. Global quantities as a function of the control variable T_{CMB} for convection with different internal heating modes, $R = 0$, 5, 10 shown in the left hand, middle and right hand column of frames respectively. Open and filled in symbols are for BA and EBA cases respectively. The top row of frames (a,b,c) shows the volume averaged viscosity. The second row (d,e,f) shows the root-mean-squared velocity. The horizontal average heatflow value through the top boundary is given the third row (g,h,i). The fourth row (j,k,l) shows the volume averaged temperature.

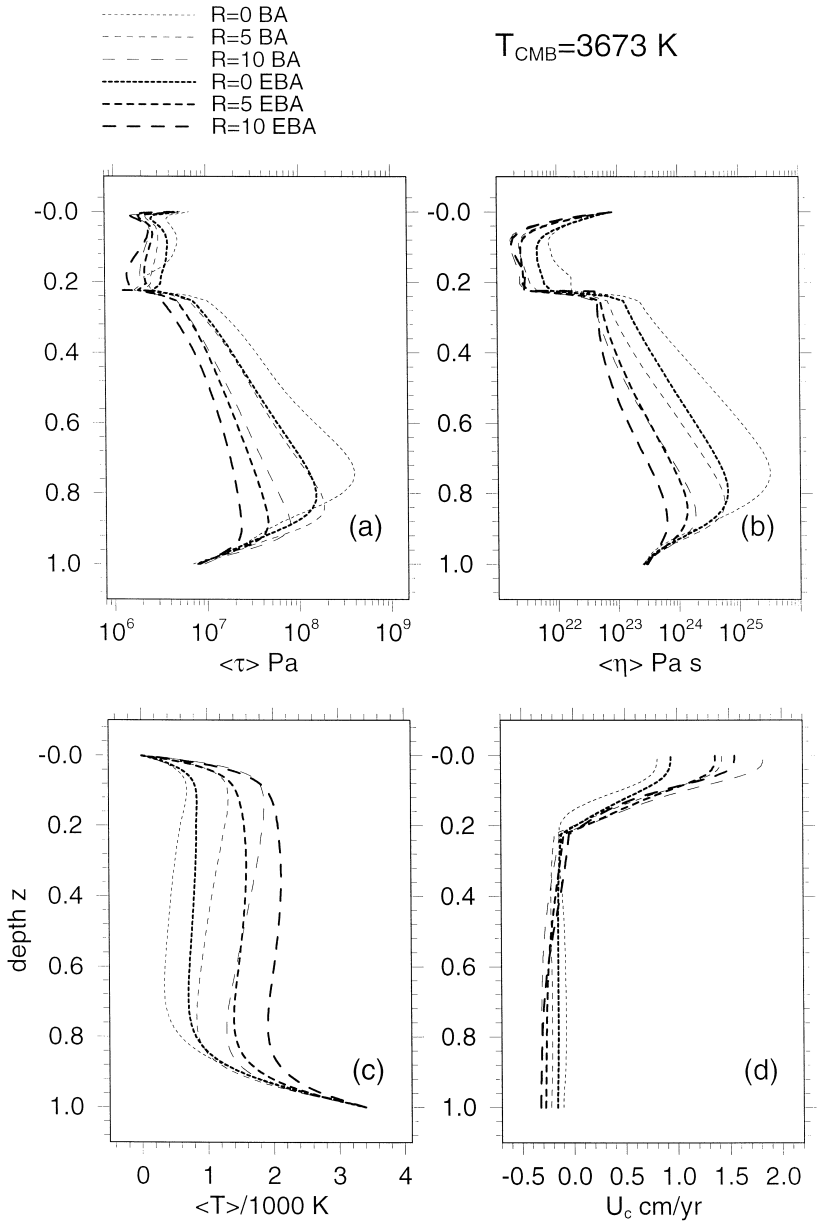

Fig. 6. One-dimensional depth distribution of the second invariant of the deviatoric stress (a), effective viscosity (b), temperature (c) and horizontal velocity. Quantities shown in (a,b,c) are horizontally averaged values. (c) shows a vertical cross-section of horizontal velocity values at $x = 1.25$, halfway the domain.

dient $\alpha(z)D(\langle T\rangle + T_0)$ for various T_{CMB} and internal heating values. For β positive the temperature gradient is superadiabatic, while a negative β denotes subadiabaticity. We observe that a rather thick and strong superadiabatic layer persists in the bottom 700 km of the model mantle, with the superadiabatic gradient reaching 5 K/km above the CMB. Above this superadiabatic layer the gradient is slightly subadiabatic, greater than -0.4 K/km. The superadiabatic layer is thicker for a purely basal-heating con-

figuration. We investigated the effect of a sharp decrease of $\alpha(z)$ in the mid-lower mantle (Chopelas, 1996) and found only small deviations in $\langle T(z)\rangle$ and $\beta(z)$ with respect to the case with continuous $\alpha(z)$. It appears that all the effects are due to the steep viscous stratification of the rheology, which renders the lower mantle sluggish and promotes a superadiabatic regime.

To put our results in perspective with classical results of Nu–Ra number relations, we have calculated an effective Ra number. The relationship between T_{CMB} and this effective Ra number Ra_E, based on the volumetrically averaged viscosity $\langle\eta\rangle$, is shown in Fig. 8. It is surprising that the effective Ra number Ra_E for the basal heating cases are quite low, between 7000 (Boussinesq) and 100,000 (extended Boussinesq). Nonetheless, the entire mantle is still able to transport heat out by convection because of the vigorous circulation in the upper mantle (see Fig. 3), as compared to the sluggish flow in the lower mantle. The effective Ra number increases with dissipation and internal heating because of the higher interior temperature. For this range of rheological parameters, the highest Ra_E reached is around 6×10^5. As discussed in the work of van Keken et al. (1994), the effective Ra number of the mantle may lie considerably below 10^6 because of the large volume of the Earth's lower mantle which may be endowed with a strongly pressure-dependent rheology, a decreasing thermal expansivity with depth (Chopelas and Boehler, 1992) and an increasing thermal conductivity with depth (Anderson, 1987).

The proverbial Nu vs. Ra number relationship has been used as a cornerstone for the thermal evolution of planets (e.g., Stevenson et al., 1983). But this relationship has been based on constant viscosity boundary layer theory (Turcotte and Oxburgh, 1967) which has been simplified by using a convective feedback mechanism based on temperature-dependent viscosity (Mc Kenzie and Weiss, 1975; Sharpe and Peltier, 1978). In Fig. 9, we show the Nu vs. Ra_E relationship for this type of depth-dependent composite rheology. We see here the distinct difference between the $Nu(Ra_E)$ curves for this type of rheology and those associated with a constant viscosity (e.g., Olson and Corcos, 1980; Jarvis and Peltier, 1982). The dependence of Nu on Ra_E is very weak, especially for the internally heated cases. The power-law indices of the Nu (Ra_E) curves for internal heating lie around 0.1. For basal heating the power law indices are higher, around 0.2. The flattening of the Nu(Ra) curve is due to the lower mantle following the upper mantle in a passive way. This is in contrast with the non-layered case with purely T dependent rheology in the whole mantle, where a stagnant-lid regime develops, following the underly-

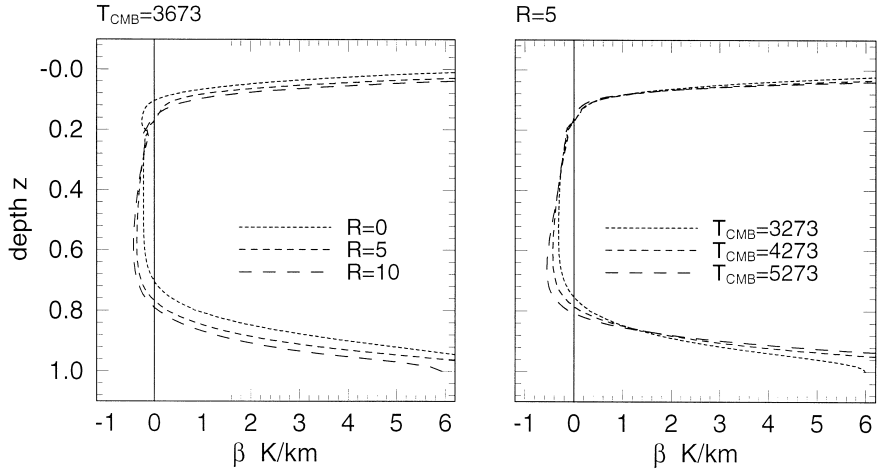

Fig. 7. Depth distribution of the index of non-adiabaticity $\beta(z)$ across the mantle, computed from the horizontally averaged geotherm, showing the deviation of the geothermal gradient from the local adiabatic gradient. (a) shows results for a fixed value of the control parameter T_{CMB} and different values of the internal heating mode $R = 0, 5, 10$. (b) shows results for a fixed values of R and a range of $T_{CMB} = 3273, 4273, 5273$ K.

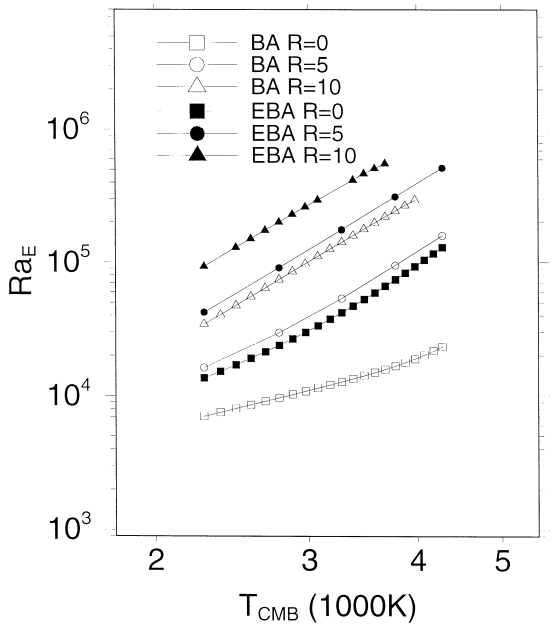

Fig. 8. Effective Ra number based on the volume averaged viscosity as a function of T_{CMB}, for different heating modes $R = 0$, 5, 10 and both BA (open symbols) and EBA (filled symbols).

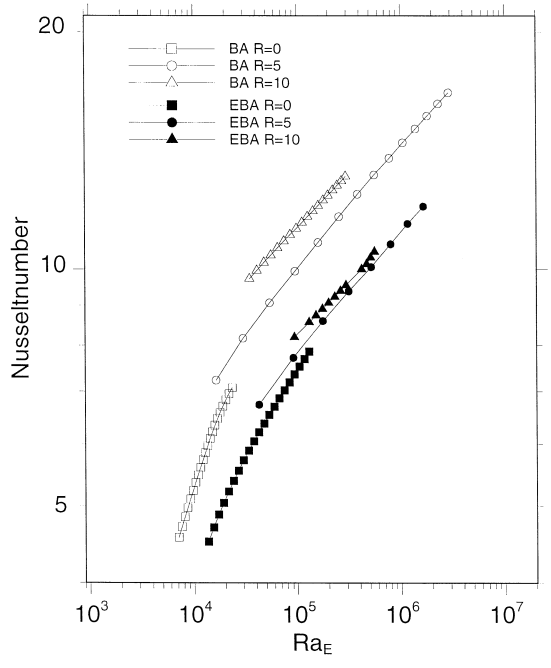

Fig. 9. Nu number vs. effective Ra number for different internal heating modes ($R = 0$, 5, 10) and BA and EBA models.

ing dynamics. In other planetary bodies such as Venus and Mars, there may exist two distinct regions with passive tendencies, reacting to an active dynamic interior.

4. Implications for planetary evolution

We can employ this approach of using the T_{CMB} as a control parameter of studying thermal evolution of planets with composite depth-dependent rheology. This scheme of things is portrayed in Fig. 10 which shows a trajectory of a hypothetical path, taken in the course of planetary evolution, on the plane prescribed by T_{CMB} and the internal heating number R used as a parameter in our models. R is a decreasing function of T_{CMB} during secular cooling due to the radioactive decay implicit in H which dominates the effect of decreasing T_{CMB} in the expression for R given in Table 2. We note that the trajectory along the T_{CMB} axis may depend upon the possibilities of temperature buffering of the CMB by chemical reactions (Knittle and Jeanloz, 1991). In general, T_{CMB} is likely to decrease with time because of core-cooling by the overlying mantle circulations (Steinbach et al., 1993), although the radioactivity inside the core may play a role in slowing down the cooling (Breuer and Spohn, 1993). Our results have been obtained by a steady-state approach and time-dependent studies,

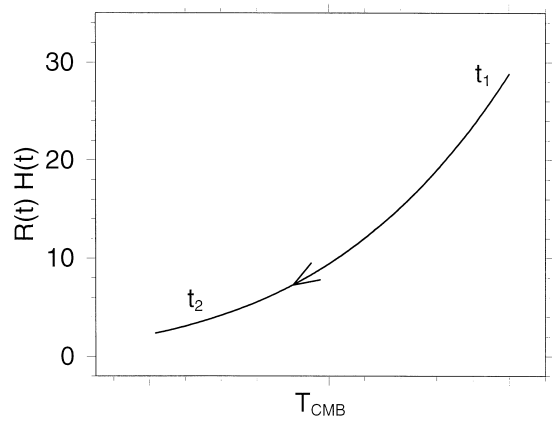

Fig. 10. Schematic diagram of the internal heating rate vs. T_{CMB}. The vertical axis indicates plausible values of the internal heating term in the energy equation including decaying radiogenic heating. The time-arrow indicates the possible direction of the evolution during secular cooling of the Earth. t_2 indicates the present, t_1 indicates the Archaean.

as were done for constant viscosity by Hansen et al. (1992), are necessary to corroborate these results.

From this study, we may surmise that all planets must have their own $Nu(Ra_E)$ curves because of (1) differences in the viscosity stratification with depth, (2) differences in the heights of the phase transitions, as in the case of Mars, in which the phase transitions lie close to the Martian CMB (e.g., Breuer et al., 1997), and (3) differences in the surface boundary conditions and the presence or absence of plate tectonics. Besides these effects, melting may also greatly modify the thermal evolution (Vlaar et al., 1994). These are important considerations to account for in planetary evolution and one cannot simply employ a simple scaling relationship in parameterized convection.

5. Conclusions and remarks

The primary issue addressed in this paper is the influences of changing convective vigor in the case of complicated mantle rheology with a strong vertical stratification. This is investigated by varying the T_{CMB}, used as a control variable, in the range 2273 to 5573 K. We have found that the usage of the T_{CMB} does allow one to study the effects on the thermal–mechanical structure inside planetary interiors. The effects of both dissipation and internal heating are found to be quite important. Both factors tend to increase the interior temperature of the convection cell and reduce both the viscosity maximum and the stress fields in the lower mantle. The effects of depth-dependent viscosity are to create a relatively thick (around 700 km), superadiabatic layer at the bottom third of the lower mantle, similar to the mean-field results of Quareni et al. (1986).

Another major point that has been clearly revealed is the significant influence exerted by the depth-dependence of mantle rheology on the scaling relationship between the global heat-transfer and the effective Ra number. The power-law index in the traditional $Nu(Ra_E)$ relationship is found to be greatly reduced in the face of a pressure-dependence in a temperature- and pressure-dependent Newtonian and non-Newtonian composite rheology. Our results underscore the importance to consider this type of composite rheology in thermal evolution studies. Planetary evolution with the added ingredient of pressure-dependent rheology would occur with a much smaller rate of cooling than in the common parameterized convection models based solely on temperature-dependent viscosity.

Acknowledgements

We acknowledge discussions with Shun Karato and Ondřej Čadek about the issue of the superadiabatic geothermal gradient in the lower mantle and insightfull comments by two anonymous reviewers. This research has been supported by NATO and the geophysics program of the National Science Foundation.

References

Anderson, D.L., 1987. A seismic equation of state: II. Shear properties and thermodynamics of the lower mantle. Phys. Earth Planet. Inter. 45, 307–323.

Balachandar, S., Yuen, D.A., Reuteler, D.M., 1992. Time-dependent three-dimensional compressible convection with depth-dependent properties. Geophys. Res. Lett. 19, 2247–2250.

Balachandar, S., Yuen, D.A., Reuteler, D.M., 1996. High Rayleigh number convection at infinite Prandtl number with weakly temperature-dependent viscosity. Geophys. Astrophys. Fluid Dyn. 83, 79–117.

Breuer, D., Spohn, T., 1993. Cooling of the Earth, Urey ratios, and the problem of potassium in the core. Geophys. Res. Lett. 20, 1655–1658.

Breuer, D., Yuen, D.A., Spohn, T., 1997. Phase transitions in the Martian mantle: implications for partially layered convection. Earth Planet. Sci. Lett. 148, 457–469.

Bunge, H.-P., Richards, M.A., Baumgardner, J.R., 1996. Effect of depth-dependent viscosity on the planform of mantle convection. Nature 379, 436–438.

Bunge, H.-P., Richards, M.A., Baumgardner, J.R., 1997. A sensitivity study of three-dimensional spherical mantle convection at 10^8 Rayleigh number: effects of depth-dependent viscosity, heating mode, and an endothermic phase change. J. Geophys. Res. 102 (11), 11991–12008.

Chopelas, A., 1996. Thermal expansivity of lower mantle phases MgO and $MgSiO_3$ perovskite at high pressure derived from vibrational spectroscopy. Phys. Earth Planet. Inter. 98, 3–15.

Chopelas, A., Boehler, R., 1992. Thermal expansivity of the lower mantle. Geophys. Res. Lett. 19, 1983–1986.

Christensen, U.R., 1984. Convection with pressure and temperature dependent non-Newtonian rheology. Geophys. J.R. Astr. Soc. 77, 343–384.

Dziewonski, A.M., Anderson, D.L., 1981. Preliminary reference earth model (PREM). Phys. Earth Planet. Inter. 25, 297–356.

Goetze, C., Kohlstedt, D.L., 1973. Laboratory study of dislocation climb and diffusion in olivine. J. Geophys. Res. 78, 5961–5971.

Gurnis, M., 1989. A reassessment of the heat transport by variable viscosity convection with plates and lids. Geophys. Res. Lett. 16, 179–182.

Hansen, U., Yuen, D.A., 1994. Effects of depth-dependent thermal expansivity on the interaction of thermal–chemical plumes with a compositional boundary. Phys. Earth Planet. Inter. 86, 205–221.

Hansen, U., Yuen, D.A., Malevsky, A.V., 1992. A comparison of steady-state and strongly chaotic thermal convection at high Rayleigh number. Phys. Rev. A 46, 4742–4755.

Hansen, U., Yuen, D.A., Kroening, S.E., Larsen, T.B., 1993. Dynamical consequences of depth-dependent thermal expansivity and viscosity on mantle circulations and thermal structure. Phys. Earth Planet. Inter. 77, 205–223.

Holland, K.G., Ahrens, T.J., 1997. Melting of $(Mg, Fe)SiO_4$ at the core–mantle boundary of the Earth. Science 275, 1623–1625.

Ita, J., King, S.D., 1994. Sensitivity of convection with an endothermic phase change to the form of governing equations, initial conditions, boundary conditions, and equation of state. J. Geophys. Res. 99 (15), 15919–15938.

Jarvis, G.T., Mc Kenzie, D.P., 1980. Convection in a compressible fluid with infinite Prandtl number. J. Fluid Mech. 96, 515–583.

Jarvis, G.T., Peltier, W.R., 1982. Mantle convection as a boundary-layer phenomenon. Geophys. J.R. Astr. Soc. 68, 385–424.

Karato, S., 1992. On the Lehmann discontinuity. Geophys. Res. Lett. 19, 2255–2258.

Karato, S., 1997. Phase transformations and rheological properties of mantle minerals. In: Crossley, D.J. (Ed.), Earth's Deep Interior. Gordon & Breach, London, pp. 223–272.

Karato, S., Li, P., 1992. Diffusion creep in perovskite: implications for the rheology of the lower mantle. Science 255, 1238–1240.

Karato, S., Rubie, D.C., 1997. Toward an experimental study of deep mantle rheology: a new multianvil sample assembly for deformation studies under high pressures and temperatures. J. Geophys. Res. 102, 20111–20122.

Karato, S., Wu, P., 1993. Rheology of the upper mantle: a synthesis. Science 260, 118–771.

Karato, S., Zhang, S., Wenk, H.R., 1995. Superplasticity in Earth's lower mantle: evidence from seismic anisotropy and rock physics. Science 270, 458–461.

King, S.D., 1995. Radial models of mantle viscosity: results from a genetic algorithm. Geophys. J. Int. 122, 725–734.

King, S.D., Gable, C.W., Weinstein, S.A., 1992. Models of convection-driven tectonic plates: a comparison of methods and results. Geophys. J. Int. 109, 481–487.

Knittle, E., Jeanloz, R., 1987. The activation energy of the back transformation of silicate perovskite to enstatite. In: Manghnani, M., Syono, Y. (Eds.), High-Pressure Research in Geophysics and Geochemistry. AGU, Washington, DC, pp. 243–250.

Knittle, E., Jeanloz, R., 1991. Earth's core–mantle boundary: results of experiments at high pressures and temperatures. Science 251, 1438–1443.

Lambeck, K., Johnston, P., Smither, C., Nakada, M., 1996. Glacial rebound of the British Isles: III. Constraints on mantle viscosity. Geophys. J. Int. 125, 340–354.

Larsen, T.B., Yuen, D.A., 1997. Ultrafast upwelling bursting through the upper mantle. Earth Planet. Sci. Lett. 146, 393–400.

Machetel, P., Weber, P., 1991. Intermittent layered convection in a model mantle with an endothermic phase change at 670 km. Nature 350, 55–57.

Machetel, P., Yuen, D.A., 1989. Penetrative convective flows induced by internal heating and mantle compressibility. J. Geophys. Res. 94, 10609–10626.

Machetel, Ph., Thoraval, C., Brunet, D., 1995. Spectral and geophysical consequences of 3-D spherical mantle convection with an endothermic phase change at the 670 km discontinuity. Phys. Earth Planet. Inter. 88, 43–53.

Mc Kenzie, D.P., Weiss, N.O., 1975. Speculations on the thermal and tectonic history of the Earth. Geophys. J.R. Astr. Soc. 42, 131–174.

Mitrovica, J.X., Forte, A.M., 1997. Radial profile of mantle viscosity: results from the joint inversion of convection and postglacial rebound observables. J. Geophys. Res. 102, 2751–2769.

O'Connell, R.J., 1977. On the scale of mantle convection. Tectonophysics 38, 119–136.

Olson, P.L., Corcos, G.M., 1980. A boundary layer model for mantle convection with surface plates. Geophys. J.R. Astr. Soc. 62, 195–219.

Pari, G., Peltier, W.R., 1996. The free-air gravity constraint on subcontinental mantle dynamics. J. Geophys. Res. 101, 28105–28132.

Parmentier, E.M., Turcotte, D.L., Torrance, K.E., 1976. Studies of finite amplitude non-Newtonian thermal convection with application to convection in the earth's mantle. J. Geophys. Res. 81, 1839–1846.

Quareni, F., Yuen, D.A., Saari, M.R., 1986. Adiabaticity and viscosity in deep mantle convection. Geophys. Res. Lett. 13, 38–41.

Ranalli, G., 1995. Rheology of the Earth, 2nd edn. Chapman & Hall, London.

Sammis, C.G., Smith, J.C., Schubert, G., Yuen, D.A., 1977. Viscosity depth profile of the earth's mantle: effects of polymorphic phase transitions. J. Geophys. Res. 82, 3747–3761.

Schmeling, H., Jacoby, W.R., 1981. On modelling the lithosphere in mantle convection with nonlinear rheology. J. Geophys. 50, 89–100.

Sharpe, H.N., Peltier, W.R., 1978. Parameterized mantle convection and the Earth's thermal history. Geophys. Res. Lett. 5, 737–740.

Shen, G., Lazor, P., 1995. Melting of minerals under the lower mantle conditions: experimental results. J. Geophys. Res. 100 (17), 17699–17713.

Solomatov, V.S., Moresi, V.N., 1996. Stagnant lid convection on Venus. J. Geophys. Res. 101, 4737–4753.

Spohn, T., Schubert, G., 1982. Modes of mantle convection and

the removal of heat from the earth's interior. J. Geophys. Res. 87, 4682–4696.

Stacey, F.D., 1997. Bullen's seismological homogeneity parameter, η, applied to a mixture of minerals: the case of the lower mantle. Phys. Earth Planet Inter. 99, 189–193.

Steinbach, V., Yuen, D.A., 1994. Effects of depth-dependent properties on the thermal anomalies produced in flush instabilities from phase transitions. Phys. Earth Planet. Inter. 86, 165–183.

Steinbach, V., Yuen, D.A., 1997. Dynamical effects of a temperature- and pressure-dependent lower-mantle rheology on the interaction of upwellings with the transition zone. Phys. Earth Planet. Inter. 103, 85–100.

Steinbach, V., Hansen, U., Ebel, A., 1989. Compressible convection in the earth's mantle: a comparison of different approaches. Geophys. Res. Lett. 16.

Steinbach, V., Yuen, D.A., Zhao, W., 1993. Instabilities from phase transitions and the timescales of mantle evolution. Geophys. Res. Lett. 20, 1119–1122.

Stevenson, D.J., Spohn, T., Schubert, G., 1983. Magnetism and thermal evolution of the terrestrial planets. Icarus 54, 466–489.

Turcotte, D.L., Oxburgh, E.R., 1967. Finite amplitude convective cells and continental drift. J. Fluid Mech. 28, 29–42.

van den Berg, A.P., Yuen, D.A., 1996. Is the lower-mantle rheology Newtonian today?. Geophys. Res. Lett. 23, 2033–2036.

van den Berg, A.P., Yuen, D.A., 1997. The role of shear heating in lubricating mantle flow. Earth Planet. Sci. Lett. 151, 33–42.

van den Berg, A.P., Yuen, D.A., van Keken, P.E., 1991. Effects of depth-variations in creep laws on the formation of plates in mantle dynamics. Geophys. Res. Lett. 18, 2197–2200.

van den Berg, A.P., van Keken, P.E., Yuen, D.A., 1993. The effects of a composite non-Newtonian and Newtonian rheology on mantle convection. Geophys. J. Int. 115, 62–78.

van den Berg, A.P., Yuen, D.A., van Keken, P.E., 1995. Rheological transition in mantle convection with a composite temperature dependent, non-Newtonian and Newtonian rheology. Earth Planet. Sci. Lett. 129, 249–260.

van Keken, P.E., Yuen, D.A., 1995. Dynamical influences of high viscosity in the lower mantle induced by the steep melting curve of perovskite: effects of curvature and time dependence. J. Geophys. Res. 100 (B8), 15233–15248.

van Keken, P.E., Yuen, D.A., van den Berg, A.P., 1992. Pulsating diapiric flows: consequences of vertical variations of mantle creep laws. Earth Planet. Sci. Lett. 112, 179–194.

van Keken, P.E., Yuen, D.A., van den Berg, A.P., 1993. The effects of shallow rheological boundaries in the upper mantle on inducing shorter timescales of diapiric flows. Geophys. Res. Lett. 20, 1927–1930.

van Keken, P.E., Yuen, D.A., van den Berg, A.P., 1994. Implications for mantle dynamics from the high melting temperature of perovskite. Science 264, 1437–1439.

Vlaar, N.J., van Keken, P.E., van den Berg, A.P., 1994. Cooling of the Earth in the Archaean: consequences of pressure-release melting in a hotter mantle. Earth Planet. Sci. Lett. 121, 1–18.

Weertman, J., Weertman, J.R., 1975. High temperature creep of rock and mantle viscosity. Annu. Rev. Earth Planet. Sci. 3, 293–315.

Yuen, D.A., Zhang, S., 1989. Equation of state and rheology in deep mantle convection. In: Navrotsky, A., Weidner, D.J. (Eds.), Perovskites. AGU Monograph, Vol. 45, American Geophysical Union, Washington, DC, pp. 131–146.

Zerr, A., Boehler, R., 1993. Melting of $(Mg, Fe)SiO_3$ perovskite to 625 Kilobars: indication of a high melting temperature in the lower mantle. Science 262, 553–555.

Zerr, A., Boehler, R., 1994. Constraints on the melting temperature of the lower mantle from high-pressure experiments on MgO and magnesiowustite. Nature 371, 506–508.

Zhang, S., Yuen, D.A., 1995. The influences of lower-mantle viscosity stratification on 3-D spherical-shell mantle convection. Earth Planet. Sci. Lett. 132, 157–166.

Zhang, S., Yuen, D.A., 1996. Various influences on plumes and dynamics in time-dependent, compressible, mantle convection in 3-D spherical shell. Phys. Earth Planet. Inter. 94, 241–267.